Impact of powder recoating speed on built properties in PBF-LB process

N.B. When citing this work, cite the original published paper.

(article starts on next page)

10th CIRP Global Web Conference – Material Aspects of Manufacturing Processes

Impact of powder recoating speed on built properties in PBF-LB process

Laura Cordova[a,b]*, Zhuoer Chen[a]

(a) *Department of Industrial and Materials Science, Chalmers University of Technology, Göteborg, Sweden*

(b) *Department of Mechanics of Solids, Surfaces & Systems (MS3), University of Twente, Enschede, The Netherlands*

* Corresponding author. Tel.: +46(0)31-772 1271. *E-mail address:* laura.cordova@chalmers.se

Abstract

In powder bed fusion laser-beam (PBF-LB), powder deposition parameters are not commonly adjusted for different materials. In this study, the recoater speed was varied from 150 mm/s to 500 mm/s to study its influence on processability of two different powders. The 420 steel powder possesses better flowability and higher packing density than Inconel 718 at different testing speeds. This is reflected on surface roughness (S_a): Inconel 718 samples show larger variations than 420 steel ones across different locations on the build plate and under different recoating speeds. This demonstrates the necessity of accounting for powder properties for robust PBF-LB processing.

1. Introduction

Powder Bed Fusion Laser-Beam (PBF-LB) process is one of the most industrially adopted Additive Manufacturing (AM) technologies due to its versatility to create complex structures with good surface finish from Computer Aided Design (CAD) models [1]. During the PBF-LB process, thin layers of powder are deposited on a build plate and then melted by a laser beam.

The shift from rapid prototyping to production of high-performance components in highly regulated fields such as aerospace and medical required dedicated qualification of materials, machines and process [2,3]. In the meantime, various strategies are being developed to mitigate the high costs that come with using gas atomized powder, energy consumption and machine cost. In the PBF-LB process, spreading a uniform and packed layer will avoid powder bed defects, voids, segregation and overall qualities issues. The

powder behavior in terms of how it interacts with the recoating mechanism play a vital role regarding the powder bed layer quality [4]. Powder spreadability can be defined as the powder ability to spread in thin layer application.

The powder spreading during PBF-LB depends on the recoater geometry, speed, layer thickness and material. For example, Haeri *et al.* [5] developed a super-elliptic edge profile blade type spreader based on a previous study on rollers and blade spreaders in which the first ones proved to outperform at the same operating conditions. Haeri *et al.* [6] reported that according to a discrete element method (DEM) model higher spreader translational velocities result in a lower powder bed quality using polymeric powder, i.e. bed surface roughness and void fraction increases. In addition, Meier *et al.* [7] found that the powder layer quality deteriorated as particle size decreased and the cohesion between particles increased according to a discrete particle method (DPM) model. Spurek *et al.* [8] studied the link between particle size,

powder flowability and part density in SS316L and concluded that coarser particle size (28 μm < D_{50}< 38 μm) negatively affects the part density during the PBF process. Haferkamp *et al.* [9] found a linear dependency of powder layer density on the D50 of powder using monomodal powders with good flowability.

Degradation of powder during storage, handling, transport, and usage in PBF-LB systems can influence the behavior of the material [10]. Changes to the powder properties due to the reuse of material has been investigated by Cordova *et al.* [11,12], in particular the powder flowability which tends to improve with particle coarsening in PBF-LB was investigated. The spreadability of powder also depends on properties such as particle size and distribution, morphology, surface chemistry and chemical composition as studied by Cordova *et al.* [13] on a variety of commercial alloys for PBF-LB with different moisture contents.

Most of the optimization of recoating parameters were performed using simulation tools in combination with experimental validation using polymeric materials. It is necessary to build a link between recoater speed and part quality, from the perspective of powder spreadability using dedicated experiments, which leads to the optimizations of recoating parameters for PBF-LB processing of metallic powders. In this work, we evaluate the influences of recoating speed, powder flowability and their interactive effects on the spreadability of powder during the PBF-LB process and the resultant surface finish of built test pieces.

2. Materials and Methods

Pre-alloyed powders of 420 steel and Inconel 718 with D50 of 42 μm and 31 μm were supplied by Höganäs AB (Sweden). The PBF-LB experiments were conducted in an EOS M290 machine to produce horizonal blocks and powder containers as shown in Fig. 1a. The powder containers were empty inside so that recoated powder can be captured for analysis. The process parameters used to produce the samples were optimized for both materials. A volumetric energy density (Equation (1)) of $E_V = 67$ J/mm^3 was used for Inconel 718 and $E_V = 75$ J/mm^3 for 420 steel. Note that a lower $E_V = 47$ J/mm^3 was applied to the Inconel 718 containers since overheating in the container due to its geometry caused build failure in early trials. During the PBF-LB process, a layer thickness of 40 μm was applied, a stripped laser scan pattern with 67° rotation between layers was employed. The build plate was pre-heated to 80 °C.

$$E_V = \frac{P}{v \cdot h \cdot l} \tag{1}$$

where P denotes laser power, v denotes scan speed, h denotes hatch distance and l denotes layer thickness.

The powder morphology was analyzed using a FEI / Philips XL30 Environmental Scanning Electron Microscope (ESEM). The flowability behavior was studied using a revolution powder analyzer (RPA) from Mercury Scientific. An equal sample size of 110 grams of each powder composition was loaded into de drum ($d_{drum} = 50$ mm). The avalanche angle was measured using the multi-flow method

varying the rotation rate from 1 to 70 revolutions per minute (RPM) in which 75 avalanches per speed were analyzed. In general, the lowest the avalanche angle and cohesion the higher the flowability as indicated by Spierings *et al.* [14] The recoating speed can be linked to the rotation rate by using Equation (2). In this case a speed of 150 mm/s typically used for steel and nickel-based alloys was used in addition to the maximum recoating speed allowed by the PBF-LB machine of 500 mm/s. These when transformed to rotation rates are 57,29 RPM and 190,98 RPM for 150 mm/s and 500 mm/s respectively.

$$\omega = \frac{V_L}{2 \cdot \pi \cdot R} [RPM] \tag{2}$$

where ω denotes rotation rate, V_L recoating speed (linear speed) and R denotes the rotation drum radius.

The packing density of the powders in different locations of the build plate was calculated by measuring the weight of the powder entrapped in the printed container at the front, middle and back of the build plate taking as a reference the recoater initial location.

The surface roughness of printed samples was measured using a Keyence Confocal Microscope (VK 9700, Japan) model with a 10× lens. The surface roughness was measured at 5 different locations to determine the average value and relative variation, for each cube, the side faces that are perpendicular and parallel to the recoater blade are measured (Fig. 2b). When analyzing the data by the Color 3D VK-Analyzer the cutoff parameters selected were: $\lambda_s = 25$ μm and $\lambda_c= 0.8$ mm to filter out short-wavelength noise and surface waviness. In certain cases, there are invalid areas where the microscope could not find proper focus due to the presence of re-entrant features and deep vales, such areas are removed when calculating roughness parameters.
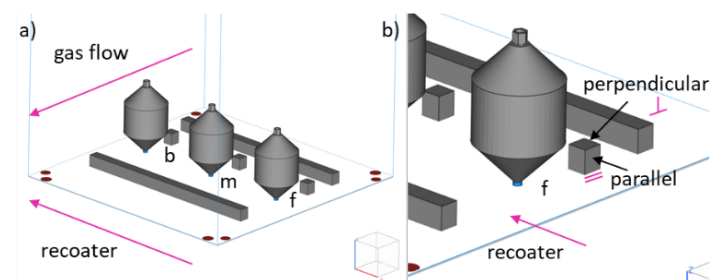

Fig. 1. (a) Overview build job with gas flow and recoater direction pointed by arrows; (b) detail on the areas of the test cubes parallel and perpendicular to the recoater direction of movement.

3. Results and Discussion

3.1. Powder properties

The spreadability of the powder depends on its properties such as particle size distribution, morphology, chemical composition, and density. The morphological features of the studied powder are shown in Figures 2b and 2c. The 420 steel powder presents a more homogenously spherical morphology with not many satellites compared to the Inconel 718 powder. The D50 of the Inconel 718 powder is lower than that of the

420 steel powder. The Inconel 718 powder contains more irregularly shaped particles and with a larger number of satellites. The differences in morphology and particle size can strongly impact the quality of parts produced by the PBF-LB process as discussed by Whiting *et. al* [15].
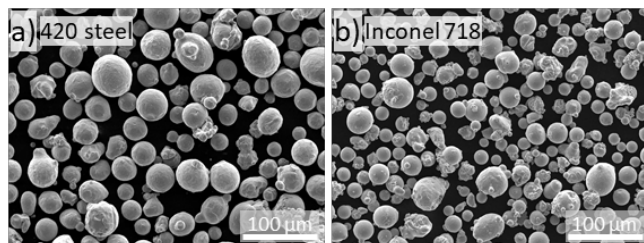

Fig. 2. Morphological features of (a) 420 steel powder and (b) Inconel 718 powder.

The results obtained with the RPA at different rotation rates reflect the influence of different powder morphology and size. Measurements on cohesion (Fig. 3a) and avalanche angle (Fig. 3b) reveal clear differences in both 420 steel and Inconel 718 powders. Both attributes increase with the rotation rate, whereas the increase in Inconel 718 powder is more significant. In the range of rotation rate from 1 – 70 RPM, 420 steel shows lower avalanche angles which is an indication of better flowability.
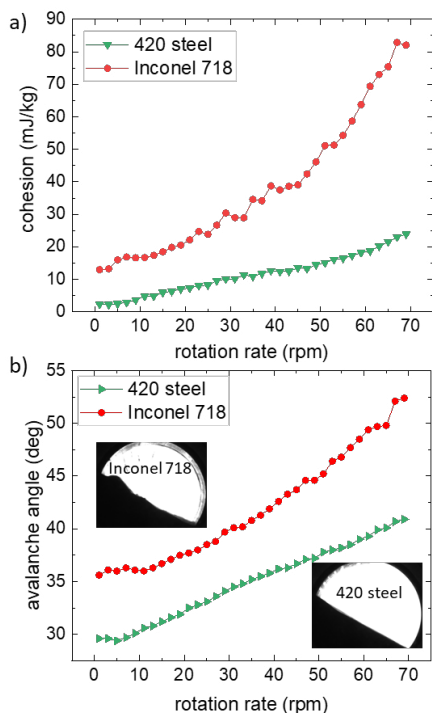

Fig. 3. RPA results of the powders on (a) cohesion and (b) avalanche angle.

3.2. PBF-LB processability at different recoating speeds

During the PBF-LB process the steel recoater blade deposits thin layers of powder on the build plate. During the first few layers of powder recoating, the uniformity in coated powder

thickness is heavily influenced by the surface roughness of the build plate. As the build progresses, the powder bed surface has a more homogenous visual appearance. In Fig. 4 the processability of 420 steel and Inconel 718 by PBF-LB is demonstrated. For both 420 steel and Inconel 718 many spatter particles were generated in the process as seen in Fig. 3a, 3b, 3e and 3f. The spatter particles are deposited on the powder bed. These can be detrimental for the part quality and lead to formation of internal defects such as pores as discussed by [16]. Furthermore, the powder containers built with 420 steel shows discoloration on surface while the cubes do not, indicating surface oxidation of the containers due to geometrical effect on heat transfer. Although not large differences can be drawn from the images of Fig. 4, it was observed a more homogenous layer deposited with recoating speed of 150 mm/s in comparison to 500 mm/s.
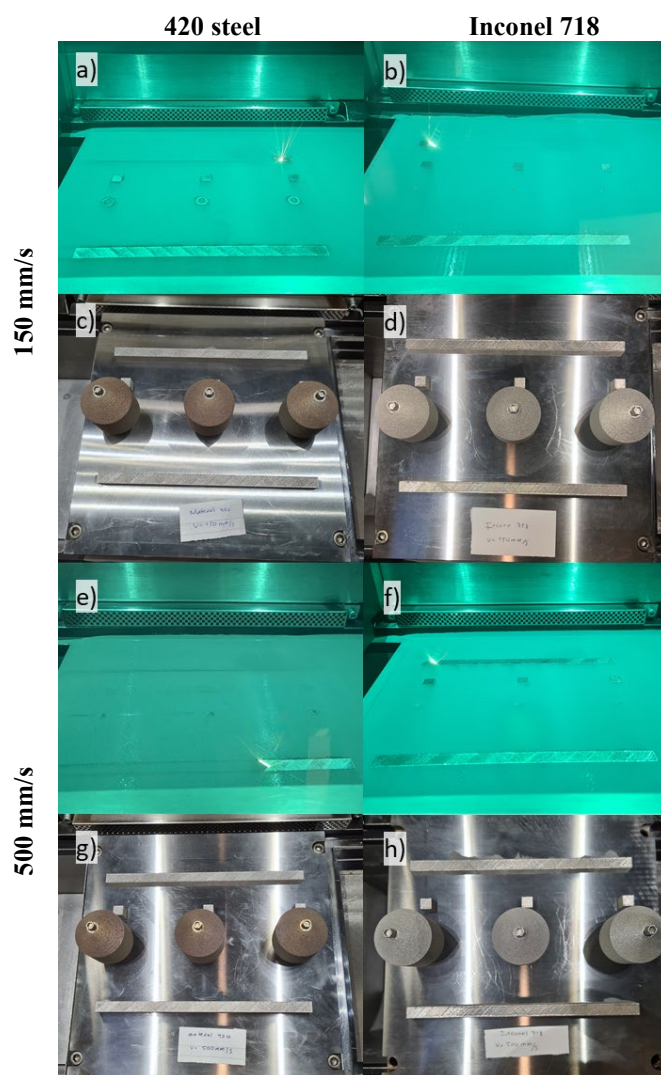
420 steel **Inconel 718**

Fig. 4. Processability by PBF-LB of 420 steel (a, c, e, g) and Inconel 718 (b, d, f, h) powder using 150 mm/s (a, b, c, d) and 500 mm/s (e, f, g, h) recoating speed.

3.3. Powder packing and distribution

The powder containers shown in Fig. 1 allowed to measure the amount of powder particles deposited at different locations of the build plate: front, middle and back at different recoating speeds. Fig. 5 shows the distribution of the packing

fraction for both materials, calculated according to Equation (3).

$$Packing\ fraction = \frac{m/V}{\rho} \qquad (3)$$

where m is the mass of powder collected from the container, V is the volume of cavity in the container by design, and ρ is the ideal density of the material. The volume occupied by powder was calculated from the design file, V= 49.5 cm^3; the ideal solid density for the 420 steel and Inconel 718 alloy were calculated as 7.75 g/cm^3 and 8.22 g/cm^3 respectively.

The 420 steel powder shows higher packing fractions at both 150 mm/s and 500 mm/s recoating speeds, and the decrease in powder packing fraction with increasing recoating speeds is less significant than that of the Inconel 718 powder. In general, both materials show good packing fractions (over 55%) at 150 mm/s recoating speed. However, upon increasing the recoating speed, the Inconel 718 powder showed a steeper decrease in packing fraction along the recoating direction (Fig. 5), which is well correlated to the high cohesion and avalanche angle tested at higher rotation speeds in RPA experiments (Fig. 3).
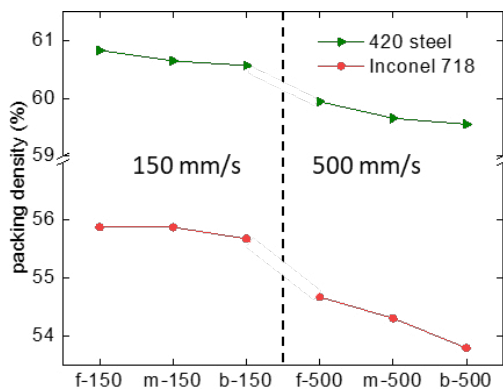

Fig. 5. Packing fractions of deposited powder of 420 steel and Inconel 718 in different locations of the powder bed.

3.4. Surface roughness

Surface roughness is not only an important aspect of product quality but also contains information about process stability in PBF-LB products [17]. Areal roughness values (S$_a$) of the printed cubes were measured on the indicated sides on Fig. 1b. The graph in Fig. 6 shows the differences in S$_a$ values measured from 420 steel and Inconel 718 samples. The 420 samples show consistently lower values in S$_a$ regardless of sample location along the recoating direction (f-front and b-back) and recoating speed. On the contrary, Inconel 718 samples show high variations in S$_a$ values and larger scatter in each measured sample. At 150 mm/s recoating speed the variation in S$_a$ with sample location is somehow repeatable on both parallel and perpendicular sides of the tested cube, i.e., higher S$_a$ at front and lower S$_a$ at the back. At 500 mm/s recoating speed, the surface roughness of Inconel samples possesses larger internal variations given inhomogeneities at the back side of the build plate. This observation agrees with the values of packing fractions presented in Fig. 5 for Inconel 718 at 500 mm/s recoating speed, which shows lower packing density influencing the homogeneity of surface roughness (Fig. 6).
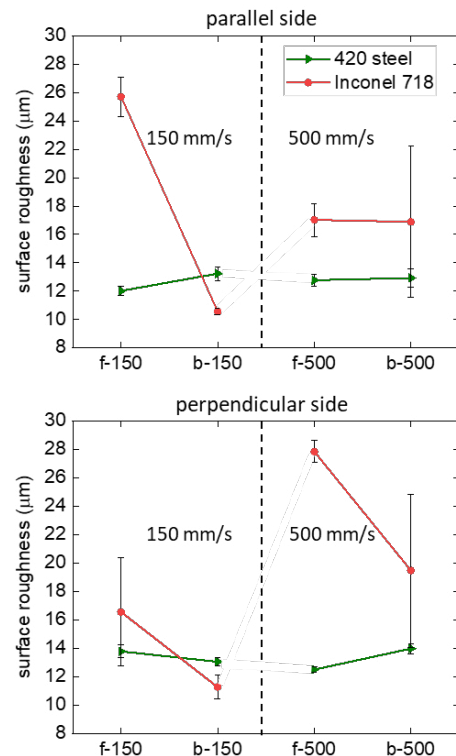

Fig. 6. Areal roughness values (S$_a$) at 150 mm/s and 500 mm/s recoating speed on (a) the parallel side to the recoater and (b) the perpendicular side to the recoater.

4. Conclusions

This work had as the main objective to show the influence of powder properties on the processability by PBF-LB process when using 150 mm/s and 500 mm/s recoating speeds. The robustness of two commercially available powders: 420 steel and Inconel 718 was assessed by measuring the flowability, powder packing density and surface roughness. It is concluded from this study:

- The 420 steel powder in comparison with Inconel 718 powder is more robust as indicated by the flowability tests. This is attributed to the coarser particle size distribution and more uniform particle shape of the 420 steel powder.
- Both materials were processed by PBF-LB without spreadability issues at 150 mm/s and 500 mm/s recoating speeds.
- The packing fractions of the powder at different locations on the build plate relative to the initial location of recoater are more variable for the Inconel 718 powder with poorer flowability in response to changes in the recoating speed.
- Changing the recoating speed for the 420 steel powder did not significantly influence the surface roughness, while for the Inconel 718 powder the surface roughness shows clear dependency on recoating speed and location along the recoating direction.

In general, it is concluded for this study that the 420 steel powder can be processed at higher recoating speeds without compromising the surface finish. The next steps are to study

the influence of recoating speed on internal defects using microscopy and images monitored from the builds using the quality assurance system connected to the PBF-LB machine.

Acknowledgements

References

[1] Gibson I, Rosen DW, Stucker B. Additive Manufacturing Technologies. Springer US; 2010. https://doi.org/10.1007/978-1-4419-1120-9.

[2] Herzog D, Seyda V, Wycisk E, Emmelmann C. Additive manufacturing of metals. Acta Mater 2016;117:371–92. https://doi.org/10.1016/j.actamat.2016.07.019.

[3] Frazier WE. Metal Additive Manufacturing: A Review. J Mater Eng Perform 2014;23:1917–28. https://doi.org/10.1007/s11665-014-0958-z.

[4] Vock S, Klöden B, Kirchner A, Weißgärber T, Kieback B. Powders for powder bed fusion: a review. Prog Addit Manuf 2019;4:383–97. https://doi.org/10.1007/s40964-019-00078-6.

[5] Haeri S. Optimisation of blade type spreaders for powder bed preparation in Additive Manufacturing using DEM simulations. Powder Technol 2017;321:94–104. https://doi.org/10.1016/j.powtec.2017.08.011.

[6] Haeri S, Wang Y, Ghita O, Sun J. Discrete element simulation and experimental study of powder spreading process in additive manufacturing. Powder Technol 2017;306:45–54. https://doi.org/10.1016/J.POWTEC.2016.11.002.

[7] Meier C, Weissbach R, Weinberg J, Wall WA, Hart AJ. Modeling and characterization of cohesion in fine metal powders with a focus on additive manufacturing process simulations. Powder Technol 2019;343:855–66. https://doi.org/10.1016/j.powtec.2018.11.072.

[8] Spurek MA, Haferkamp · Lukas, Weiss C, Adriaan ·, Spierings B, Schleifenbaum JH, et al. Influence of the particle size distribution of monomodal 316L powder on its flowability and processability in powder bed fusion. Prog Addit Manuf n.d. https://doi.org/10.1007/s40964-021-00240-z.

[9] Haferkamp L, Spierings A, Rusch M, Jermann D, Spurek MA, Wegener K. Effect of Particle size of monomodal 316L powder on powder layer density in powder bed fusion. Prog Addit Manuf 2021;6:367–74. https://doi.org/10.1007/s40964-020-00152-4.

[10] Cordova L, Campos M, Tinga T. Assessment of moisture content and its influence on laser beam melting feedstock. Proc. Euro PM 2017 Int. Powder Metall. Congr. Exhib., 2017.

[11] Cordova L, Bor T, de Smit M, Carmignato S, Campos M, Tinga T. Effects of powder reuse on the microstructure and mechanical behaviour of Al–Mg–Sc–Zr alloy processed by laser powder bed fusion (LPBF). Addit Manuf 2020;36. https://doi.org/10.1016/j.addma.2020.101625.

[12] Cordova L, Campos M, Tinga T. Revealing the Effects of Powder Reuse for Selective Laser Melting by Powder Characterization. JOM 2019;71:1062–72. https://doi.org/10.1007/s11837-018-3305-2.

[13] Cordova L, Bor T, de Smit M, Campos M, Tinga T. Measuring the spreadability of pre-treated and moisturized powders for laser powder bed fusion. Addit Manuf 2020;32:101082. https://doi.org/10.1016/J.ADDMA.2020.101082.

[14] Spierings AB, Voegtlin M, Bauer T, Wegener K. Powder flowability characterisation methodology for powder-bed-based metal additive manufacturing. Prog Addit Manuf 2016;1:9–20. https://doi.org/10.1007/s40964-015-0001-4.

[15] Whiting JG, Garboczi EJ, Tondare VN, Scott JHJ, Donmez MA, Moylan SP. A comparison of particle size distribution and morphology data acquired using lab-based and commercially available techniques: Application to stainless steel powder. Powder Technol 2022;396:648–62. https://doi.org/10.1016/J.POWTEC.2021.10.063.

[16] Lutter-Günther M, Bröker M, Mayer T, Lizak S, Seidel C, Reinhart G. Spatter formation during laser beam melting of AlSi10Mg and effects on powder quality. Procedia CIRP 2018;74:33–8. https://doi.org/10.1016/J.PROCIR.2018.08.008.

[17] Newton L, Senin N, Gomez C, Danzl R, Helmli F, Blunt L, et al. Areal topography measurement of metal additive surfaces using focus variation microscopy. Addit Manuf 2019;25:365–89. https://doi.org/10.1016/j.addma.2018.11.013.